



Chaos in a Simple Model of the Earth's Magnetic Field

By Isaac Tobin
DT222 Year 4

20th March 2009

Supervisor:
Dr. Cathal Flynn

Contents:

1 Abstract	1
2 Introduction	2
2.1 Earth's magnetic field	2
2.2 Models of the Earth's magnetic field	3
3 Theory	4
3.1 Rikitake model equations	4
3.2 Logistic map	7
3.3 Introduction to chaos	10
3.3.1 Sensitivity to initial conditions	10
3.3.2 Non-linear dynamics	11
3.3.3 Return maps	11
3.3.4 Fractals and attractors	12
3.3.5 Non-periodic and periodic behaviour	14
3.3.6 Bifurcation	15
3.4 Lorenz Attractor	17
3.5 Feigenbaum Constant	19
3.6 Correlation Dimension	20
4 Methods	22
5 Results	23
5.1 Logistic map	23
5.2 Lorenz Attractor	24
5.3 Feigenbaum Constant	26
5.4 Rikitake Attractors	27
5.5 Correlation Dimension	31
6 Discussion	32
7 Conclusion	34
8 References	—
Appendix	—

1 Abstract:

The Earth's magnetic field has been modelled many times, especially in the last few decades with the relatively recent advent of high powered computation, which allows for long term analysis of the models. Palaeomagnetic records of the Earth's magnetic field have shown that its polarity has changed hundreds of times in the past 160 million years. These reversals have no apparent regularity and are thought to be chaotic. A number of models do not show these reversals in the modelled data, however the model used in this paper shows chaotic reversals analogous to those of the Earth's magnetic field.

Many models have been derived for the Earth's magnetic field, usually focused on the magma dynamos in the core, because 97% of the Earth's magnetic field is generated from these. In this paper the Rikitake two-disc dynamo model is used as it is known to model these eddies accurately.

The Rikitake models two large eddies of molten iron in the Earth's core which both induce current on themselves and on one another. The model is approximated using a forth order Runge-Kutta. To solve the system three non-dimensional equations were derived from the model of this frictionless, coupled, two-disc dynamo. Two fixed points were derived from the system, one corresponding to the reversed polarity and the other to the normal state.

The approximated data was analysed qualitatively by examining the time series and return maps of the system as well as quantitatively by determining the fractal dimension of one of the chaotic attractors in the Rikitake model.

2 Introduction:

2.1 Earth's magnetic field

The Earth is protected from solar winds and other cosmic radiation by a large magnetic field, which is generated in the most part by the magma dynamos inside the Earth's crust. These magma flows have been modelled many times, however the Rikitake model is both simple and demonstrates the observed reversals of the North and South poles of the field.

The time between these reversals varies widely (from tens of thousands to tens of millions of years) and is thought to be chaotic. The last of these reversals, the Brunhes-Matuyama reversal, occurred approximately 780 thousand years ago.

These reversals can be of great concern, as the field strength decreases greatly during the shift from one North to the other, as it were, before a rapid recovery after the new orientation is established. This could lead to very large exposures of cosmic radiation and solar winds as well as play havoc with navigation and communication technologies. The cosmic energies incident on the Earth are visible during phenomena such as auroras borealis and australis, during which strong solar winds become deflected by the magnetic field and typically strike atmosphere above the north and south poles.

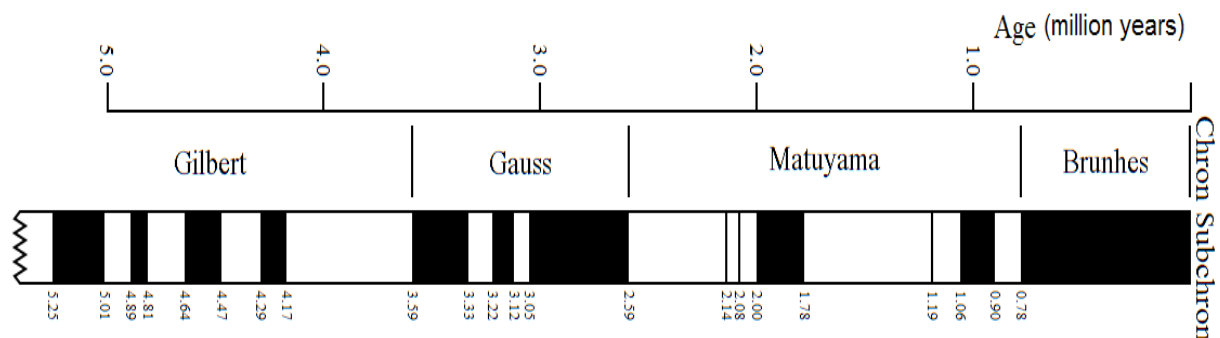


(Figure 1 – Recent geomagnetic reversals, sourced from U.S. Geological Survey)

In Figure 1 above the most recent reversals are charted as a function of time, in millions of years. Each black region represents the standard North-South arrangement and each white region the reversed order. It must be noted that this is not the extent of knowledge about past reversals, there is data charting reversals for the past 160million years, obtained from across the globe. Currently the geographic north is actually the magnetic south-pole, as observable by the north-pole on a magnet being attracted to the geographic north.

Studies of Venus show that it does not have a magnetic field like the Earth's, despite having a core iron content which must be similar to that of the Earth. The reason for this is in Venus's rotation period of 243 Earth days, which is just too slow to produce the dynamo effect which generates the field on the Earth^[1].

2.2 Models of the Earth's magnetic field

There are many contributing factors to the Earth's magnetic field, however this can be simplified for modelling. The most dominant of the factors is the magnetic field generated from the magma dynamos in the outer core region, which make up 97% of the field observed at the Earth's surface^[2].

This idea of rotating liquid iron generating a magnetic field brings forward the idea of a 'geodynamo', similar to the dynamo inside an electric generator. The rotating conductor has a current flowing through it and is surrounded by a magnetic field which induces a current on itself and on the other conductors around it.

Many models of the Earth's magnetic field have been proposed, the ones of interest here are of the magma dynamos in the Earth's outer core. The single disc model given by Bullard in 1955 performs an oscillation of characteristic nature, but no reversal of magnetic field^[3]. This models the Earth's magnetic field, however only the coupled, two disc model (Figure 2) given by Rikitake in 1958 yields the random reversals of the magnetic field^[4] which were of interest. The Rikitake model was put forward first as an elegant prototype for explaining geomagnetic polarity reversal^[5].

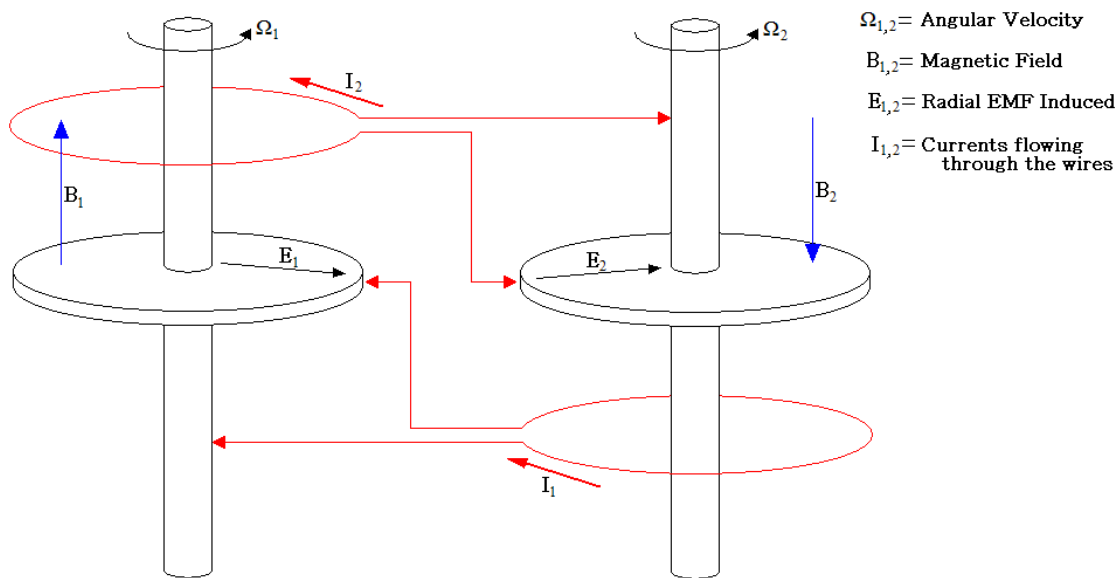


(Figure 2 – Rikitake Dynamo schematic)

As seen above, the Rikitake dynamo is made up of two, coupled, frictionless, rotating discs. There are currents, I_1 and I_2 , flowing through wires attached by brush to the discs and axis of rotation of each. There are magnetic fields B_1 and B_2 through the discs, perpendicular to rotation and they are rotating with angular velocities Ω_1 and Ω_2 which generates a mutual inductance between, and self inductance on, each disc.

The model has two fixed points (attractors) about which the system will oscillate from the vicinity of one to the vicinity of the next, which might correspond to the observed reversals in the magnetic poles.

3 Theory:

3.1 Rikitake model equations

As seen previously the Rikitake model is made up of two disc-dynamos, each with an axis of rotation, a disc and a wire, all made of the same conductive materials. These three elements form a closed circuit which makes up each of the two dynamos. The wire is in sliding contact with both the axis and the disc rim and the loop is used to form electromagnetic coupling between the two dynamos. Both discs are assumed to be far enough apart to ignore any other interaction.

To use this model a set of equations are needed to demonstrate the behaviour of the system which could then be used to show the chaotic nature of the reversals that is of interest to us, these equations are:

$$\begin{aligned}L\dot{I}_1 + RI_1 &= M\Omega_1 I_2 \\L\dot{I}_2 + RI_2 &= M\Omega_2 I_1 \\C\dot{\Omega}_1 &= G - MI_1 I_2 \\C\dot{\Omega}_2 &= G - MI_1 I_2\end{aligned}\tag{1.1}$$

Where I_i is the current through wire i , Ω_i is the angular velocity on disc i , L is the self-inductance of the dynamo, R is the resistance of the dynamo, C is the moment of inertia of the dynamo about its axis of rotation, G is the applied couple and M is the mutual inductance between the two dynamos. These were derived from Maxwell's equations in order to have a set of defining equations to model the system.

The above equations must be made into non-dimensional forms before they can be used as the model parameters for the programs and plotted, so therefore they are scaled using the substitutions:

$$\begin{aligned}\text{Time scale} &= \sqrt{\frac{CL}{GM}} \\ \text{Current scale} &= \sqrt{\frac{G}{M}} \\ \text{Angular velocity} &= \sqrt{\frac{GL}{CM}}\end{aligned}\tag{1.2}$$

From these a set of three one-dimensional dimensionless equations are derived, allowing us to plot currents and angular velocities as functions of time and against one another to generate return maps. First, using the scaling constants above:

$$\begin{aligned}I_i &= X_i \sqrt{G/M} \\ \Rightarrow \dot{I}_i &= \dot{X}_i \sqrt{G^2/LC} \\ \Omega_i &= Y_i \sqrt{GL/CM} \\ \mu &= \sqrt{CR^2/GLM}\end{aligned}\tag{1.3}$$

By substituting these values (1.3) into the system equations (1.1) then the first equation becomes:

$$\begin{aligned}
L.\dot{I}_1 + R.I_1 &= M.\Omega_1.I_2 \\
L.\dot{X}_1\sqrt{G^2/LC} + R.X_1\sqrt{G/M} &= M.Y_1\sqrt{GL/CM}.X_2\sqrt{G/M} \\
\dot{X}_1 &= -X_1\sqrt{R^2/L^2}\sqrt{G/M}\sqrt{LC/G^2} + Y_1.X_2\sqrt{M^2/L^2}\sqrt{GL/CM}\sqrt{G/M}\sqrt{LC/G^2} \\
\dot{X}_1 &= -\mu X_1 + Y_1.X_2
\end{aligned}$$

And the second equation:

$$\begin{aligned}
L\dot{I}_2 + RI_2 &= M\Omega_2 I_1 \\
L.\dot{X}_2\sqrt{G^2/LC} + R.X_2\sqrt{G/M} &= M.Y_2\sqrt{GL/CM}.X_1\sqrt{G/M} \\
\dot{X}_2 &= -X_2\sqrt{R^2/L^2}\sqrt{G/M}\sqrt{LC/G^2} + Y_2.X_1\sqrt{M^2/L^2}\sqrt{GL/CM}\sqrt{G/M}\sqrt{LC/G^2} \\
\dot{X}_2 &= -\mu X_2 + Y_2.X_1
\end{aligned}$$

We know that $Y_1 - Y_2 = A$

$$\Rightarrow \dot{X}_2 = -\mu X_2 + (Y_1 - A).X_1$$

Now we have \dot{X}_1 and \dot{X}_2 in terms of Y_1 so finally the third equation becomes:

$$\begin{aligned}
C\dot{\Omega}_1 &= G - MI_1 I_2 \\
\dot{Y}_1\sqrt{C^2}\sqrt{G^2/C^2} &= \sqrt{G^2} - X_1 X_2 \sqrt{M^2}\sqrt{G^2/M^2} \\
\dot{Y}_1 &= 1 - X_1 X_2
\end{aligned}$$

Therefore the three dimensionless equations needed to model this system are:

$$\begin{aligned}
\dot{X}_1 &= -\mu X_1 + Y X_2 \\
\dot{X}_2 &= -\mu X_2 + (Y - A)X_1 \\
\dot{Y} &= 1 - X_1 X_2
\end{aligned} \tag{1.4}$$

Where $A = \mu(K^2 - K^{-2})$

As seen from above, X_1 and X_2 are the currents flowing in either dynamo and Y is the angular velocity of the coupled discs, which is essentially the rotation of the Earth.

Setting the time derivatives to zero gives:

$$X_1 = \pm K, \quad X_2 = \pm \frac{1}{K},$$

$$Y = Y_1 = \mu.K^2, \quad Y_2 = \mu.K^{-2}$$

Using this we now find the fixed points of the system, denoted as N and R for the normal and reversed modes respectively. The parameters substituted above now must be assigned limits to further aid solutions. It has been noted from other sources that μ is typically of the order of between 10^{-3} and 10^1 and a value of $K = 2$ is the most relevant to the Earth^[6].

In order to prove these fixed points are stable we must linearise the three one-dimensional equations above (1.2). By differentiating each of the three with respect to each variable for the fixed point N we get:

$-\mu X_1 + Y X_2$	$-\mu X_2 + (Y - A)X_1$	$1 - X_1 X_2$
$wrt X_1 : -\mu + 0$	$wrt X_1 : 0 + Y - A$	$wrt X_1 : 0 - X_2 + 0$
$wrt X_2 : 0 + Y$	$wrt X_2 : -\mu + 0$	$wrt X_2 : 0 - X_1$
$wrt Y : 0 + X_2$	$wrt Y : 0 + X_1$	$wrt Y : 0 - 0$

Which is written:

$$\begin{pmatrix} -\mu & Y & X_2 \\ Y - A & -\mu & X_1 \\ -X_2 & -X_1 & 0 \end{pmatrix}$$

By substituting from the above this gives the linearised matrix:

$$\begin{pmatrix} -\mu & \mu k^2 & k^{-1} \\ \mu k^{-2} & -\mu & k \\ -k^{-1} & -k & 0 \end{pmatrix}$$

It is interesting to note that the model can be a dissipative system, because the divergence of the vector field, also called the trace of the Jacobian matrix, is always negative for $\mu > 0$. The Jacobian matrix is the matrix of first order partial derivatives above, which describes a tangential plane to the three 1-dimensional functions^[7].

To determine the stability of the fixed points the eigenvalues for this matrix must be found. To find the eigenvalues we have to show that:

$$\det \begin{pmatrix} a - \lambda & b & c \\ d & e - \lambda & f \\ g & h & i - \lambda \end{pmatrix} = 0$$

The determinant of this linearised matrix is:

$$(\mu+\lambda)((\mu+\lambda)(-\lambda))+((k)(k))-\mu k^2((\mu k^{-2})(\lambda)-(k)(-k^{-1}))+k^{-1}((\mu k^{-2})(-k)+(\mu+\lambda)(k^{-1}))$$

$$\Rightarrow -\lambda^3 - 2\mu\lambda^2 - 2\mu k^2 - 2\mu k^{-2} - \lambda k^2 - \lambda k^{-2}$$

Solving for λ -2μ , $i\sqrt{k^2 + k^{-2}}$ and $-i\sqrt{k^2 + k^{-2}}$ are found to be eigenvalues of the matrix. This is also true for the fixed point R yielding another set of eigenvalues. Therefore there is one negative real and two complex conjugate eigenvalues, this shows that the fixed point is unstable. By the same method the fixed point R is found to also be unstable^[8].

3.2 Logistic Map

The logistic map is one of the simplest methods of demonstrating periodic orbits and chaotic behaviour in dynamical systems. The reason for examining this system in this paper is to initially familiarise the reader with the behaviour of a simple non-linear system and the periodic and chaotic natures observable for certain values of λ .

$$x_{n+1} = \lambda x_n(1 - x_n) \quad (1.5)$$

The logistic map is such an easy to use example of these behaviours because it is given by a simple iterative formula shown above (1.5), it only deals with one variable (x), and is easily calculated by hand. The limiting factors in the equation are that λ lies between 0 and 4 and x_n lies between 0 and 1. For values other than these the system can yield negative number results and this isn't desired in this analysis.

For λ values less than 1 the equation decays to zero incrementally, therefore the system has an attractor at zero for all values of λ less than 1. It is also notable that as the value of λ increases the peak of the parabola increases as $\lambda/4$, up to its maximum height of 1.

Now, take a value of $\lambda = 1.4$ and picking any initial x value that is non-zero, because an x value of zero will remain zero for all iterations. Iterating from this initial x a fixed point is reached after a time at an x value of 0.286. This is an example of a period one fixed point attractor; regardless of the initial point taken, the system will be attracted to this one fixed point. At this point it is worth noting that a simple way of identifying the fixed point for any $\lambda < 3$ can be found simply by rewriting (1.5), when at a fixed point $x_{n+1} = x_n$

$$\Rightarrow x = \lambda x(1 - x)$$

$$\Rightarrow \frac{1}{\lambda} = (1 - x)$$

$$\Rightarrow x_{fixed} = \frac{\lambda - 1}{\lambda}$$

When $\lambda > 3$ this is no longer true as there is no longer only one stable fixed point. Now the system will be attracted to one of the two (or more) stable fixed points. Using $\lambda = 3.4$ as an example, x iterates towards one of the two stable fixed points and once it reaches one of them it oscillates between the two. Now the attractor of the system is not just a single point, but an attractor consisting of two periodic points^[9]. Attractors will be discussed in detail later in section 3.3.4 as will the process of this doubling of stable fixed points which is called bifurcation and is discussed in detail in section 3.3.6.

The number of stable fixed points in a system for a set of parameters is called the period of the attractor. The period should be thought of as the number of iterations needed for a system to return to its original state.

At a value close to $\lambda = 3.5$ the number of stable fixed points doubles once again to four stable fixed points (Figure 3). These bifurcations occur at various values of λ , and with changing values λ the value x_n of the fixed points change. These changes are mapped later in Figure 7 on a bifurcation diagram.

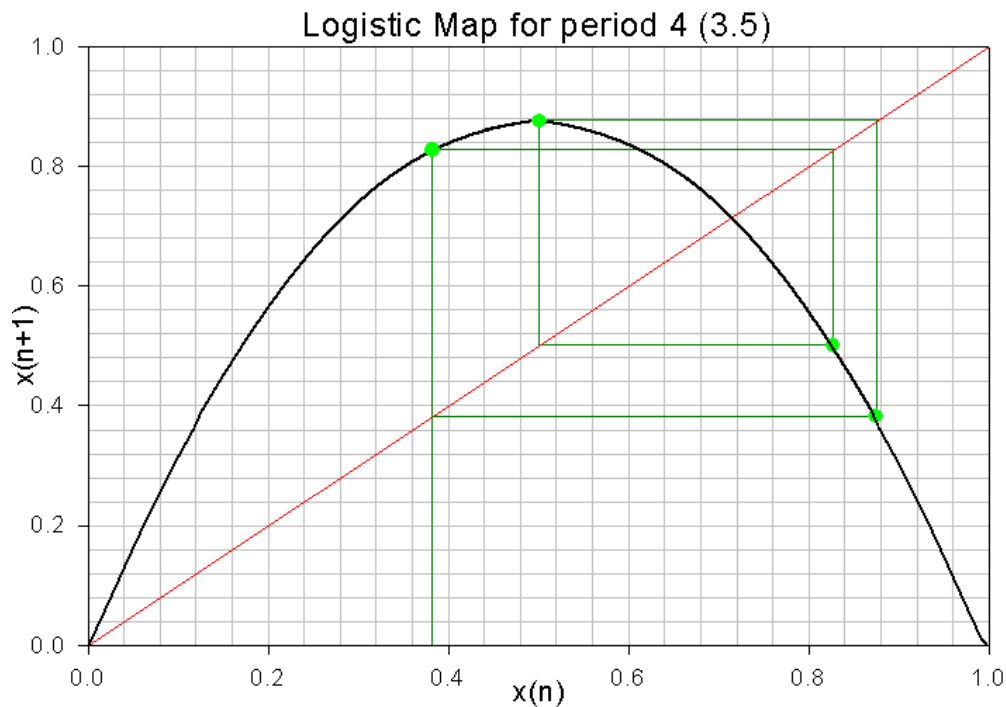


(Figure 3 – Example logistic map, showing period 4)

The $x_{n+1} = x_n$ line (red line), sometimes called the identity line. Drawing a vertical line from the x_n position of one of the stable fixed points, say $x_n = 0.383$, and drawing a line horizontally from this point to the identity line, before drawing a line vertically down, gives the next point, $x_n = 0.827$ which is the next stable fixed point.

By drawing another horizontal line from this point to the identity line and up to the next stable fixed point, $x_n = 0.501$, and from this to the next, $x_n = 0.875$, and back to the original fixed point the periodicity of the system is observed. Each of the pairs of lines drawn shows an iteration of the system.

If any other point in x_n was picked, in Figure 3, and translated similarly (iterated in the formula), one of the four fixed points would eventually be reached, after a number of iterations, and then the system would then oscillate between the four stable fixed points of this attractor.

Increasing λ further a value would be reached where period 8, then period 16, then period 32, 64, 128... would be observed. Eventually the system would have an infinitely large period and become chaotic (Figure 4), the system is found to be chaotic at a value above $\lambda \approx 3.6$.

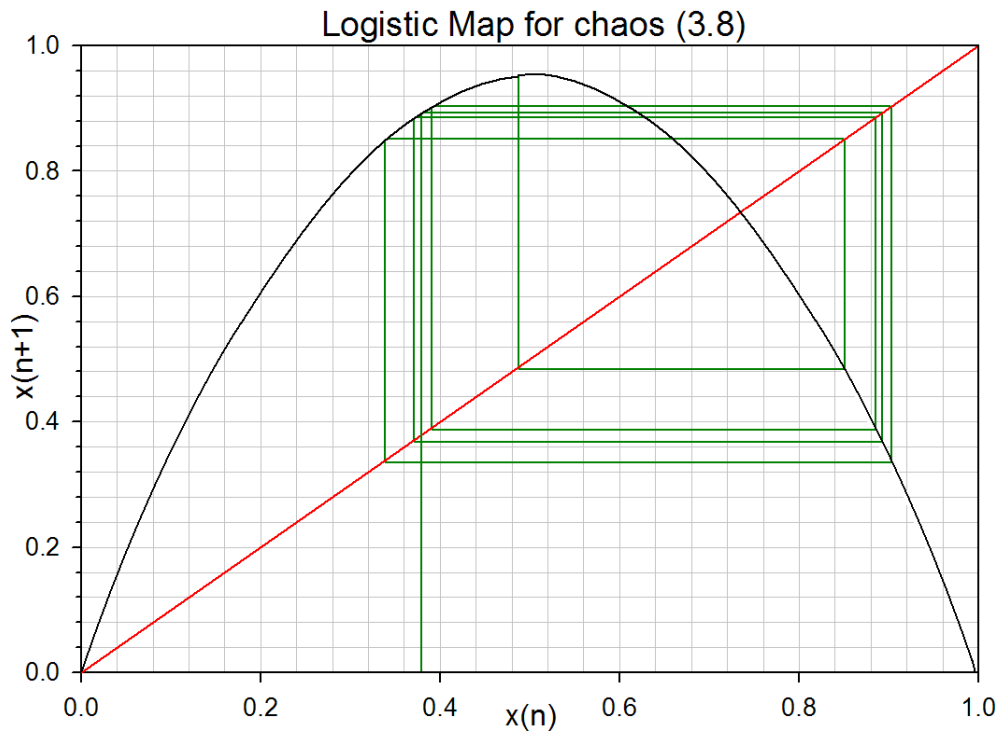


(Figure 4 – Example logistic map, showing chaos)

Now when a point is picked for x_n the iterations will not converge on a fixed point as there are no stable fixed points to be attracted to, so now if a value of x_n of 3.9 is picked the system will iterate around the identity line infinitely, showing chaotic behaviour. Chaos will be discussed in detail in the following sections and this example should be remembered as it is an ideal example of chaotic behaviour.

3.3 Introduction to chaos

3.3.1 Sensitivity to initial conditions

Chaos in everyday language means disorder and confusion, in the scientific sense which it is used to describe the behaviour of systems in this paper it does have a certain amount of disorder, however there is a lot more to it than just disarray. In order for a system to be chaotic it must be a non-linear dynamic system.

It is now well known that chaos is an everyday part of nature, however it is only relatively recently that chaotic systems have been recognized for their potential and their widespread presence in both natural and man-made worlds. Chaos theory when used to describe a dynamic system, like the Lorenz or Rikitake models, states that a microscopic change in the initial conditions of the system can produce macroscopic change in the outcome of the system. There is also inherent unpredictability in chaotic systems, over a great many repeats of the same cycle for a chaotic system the same outcome may never be observed. This gives an uncertainty in results taken over a small time which leads to large times being necessary to ensure no pattern will be missed which would eventually emerge from the seemingly random or chaotic data.

To take a very simple example of sensitivity to initial conditions and pattern less data imagine a magnetic pendulum hanging above a grid (Figure 5) with an equilibrium point at the centre of the grid. There are four magnets positioned on the grid at diagonals around the equilibrium point of the pendulum.

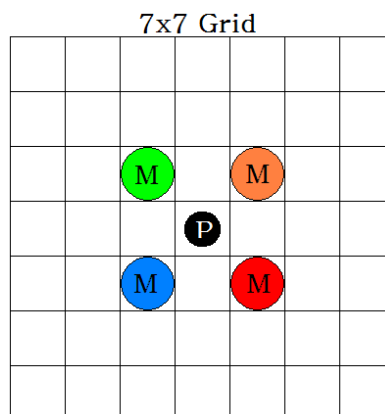


(Figure 5 – Pendulum experiment, a simple example of chaos in a system)

If the pendulum is released in any box on the grid it will eventually come to rest over one of the magnets on the board, once it has the initial box is coloured depending on which magnet it stopped on. This is repeated for all of the boxes and the grid is examined. No pattern will be observable, now the experiment is repeated for each of the boxes a second time. This time some of the boxes on the grid will have different colours to before and still no pattern will be observable.

Regardless of how many times the experiment is repeated or how large you make the grid (while keeping the four magnets at a fixed aspect ratio) no pattern will emerge from the system and the outcome can never be predicted accurately, so the system is said to be chaotic. This is a very simple example and can be easily modeled on a computer but it gives a good physical interpretation to what a chaotic system is.

3.3. 2 Non-linear dynamics

A dynamical system may be defined as a deterministic method for evolving the state of a system through time^[10]. The term deterministic means that a system outcome can be determined if the initial conditions of the system are precisely known because the outcome depends completely on the initial state of the system. It is not possible to know the initial state of the system exactly as the measurements will have an uncertainty, this uncertainty then grows exponentially in the system over time such that the outcome becomes unpredictable.

By contrast a stochastic process is non-deterministic, the outcome is dependant not only on the initial state but on some other factor which is typically called a random element. This means they are unrepeatable processes which gives them a more random nature (the word stochastic meaning random).

Everyday examples of dynamical systems are weather systems and insect populations which can be modelled to give predictions over time. It is common to see a continuous time dynamical system referred to as a flow as the path of the solutions is roughly analogous to the path followed by flowing fluids.

A system is known to be unstable when the distance between two neighbouring points in xyz-space increases exponentially with time rather than converge on an attractor or maintain a constant distance. Even when the initial distance between the two is negligible they will quickly move away from one another in an unstable system, such that the distance is no longer negligible after a short time. Such complex non-periodic motions in deterministic systems are called chaos.

Before the advent of computers modelling complex dynamical systems was almost impossible due to the huge amount of calculation necessary over the large number of iterations.

In the case of the Rikitake model the system is 3 dimensional, which, although more complex than the simple iterative equation for the logistic map, is easier than the four dimensional dynamical systems which are also modelled. The Rikitake model also only has two parameters, both of which have relatively small limiting values imposed by realistic limits for the Earth.

3.3. 3 Return maps

A 2-dimensional plot of, for example, x vs y of an attractor is called a return map, this map shows the path taken through one plane of the attractor being modelled. By plotting a 2-d plane of the attractor under examination the periodic or chaotic behaviour of the attractor can be analysed, sometimes a lot easier than by analysing the time series or 3-dimensional plots of the same data. For this reason return maps were used in this paper to demonstrate the repetitive structure of the attractors analysed.

3.3.4 Fractals and attractors

Fractals are all around us in the natural and man made world, in the past few decades they have been used to describe a great many phenomena from the length of coastlines, tree branching and lightning forks.

A fractal is the term given to an object which is, thinking of fractals in the simplest form, self similar. That is, it possesses symmetry across scale^[11] so that as you magnify any section of the object it will be similar to the previous view (Figure 6).

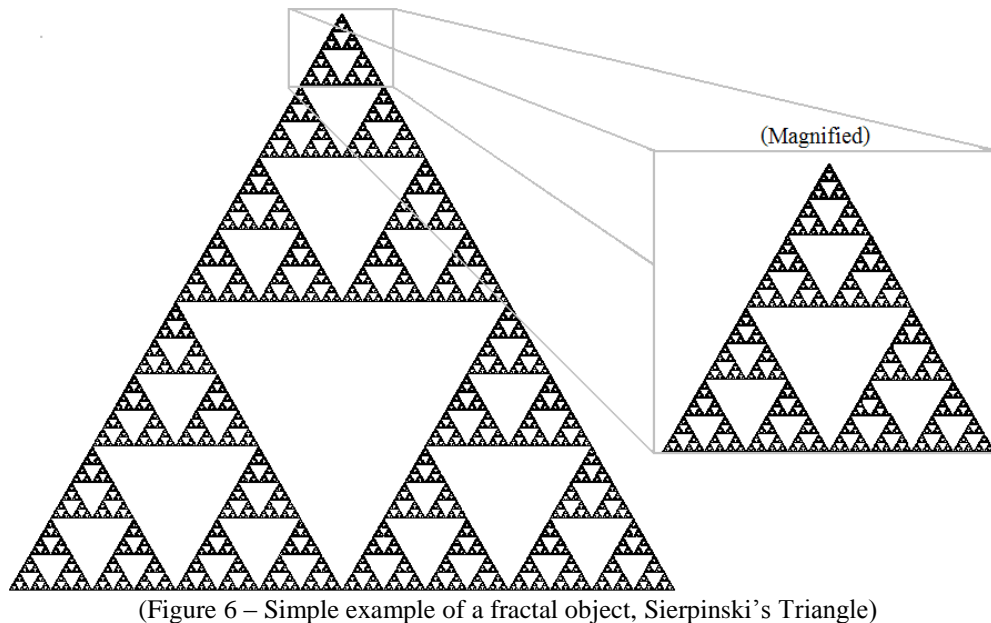


(Figure 6 – Simple example of a fractal object, Sierpinski's Triangle)

A simple way of describing a fractal is to call it an elegant geometric pattern that looks the same regardless of any change in scale, this is simply repeating what was said above but in a different way, because fractal dimensions are not something which we are often thought or often think about and so can require serious consideration to gain an understanding.

Attractors have been mentioned before, briefly, a non-chaotic attractor is generally made up of points or cycles, depending on the type of system under analysis. They will be almost unaffected in the long term by differences in initial setup, as they will always be drawn back to the attractor.

In this paper the terms strange attractor and chaotic attractor are used to mean the same thing. However some authors will use them to mean separate things. In their writings a chaotic attractor will be one in which two neighboring trajectories will diverge exponentially over time. Whereas a strange attractor would be defined by its geometrical structure, i.e. if it has a fractal structure, in their definition a strange attractor wouldn't necessarily show sensitivity to initial conditions^[12]. Therefore in their writings all chaotic attractors would be strange but not all strange attractors would be chaotic.

There are many ways to define a strange attractor, two apt definitions are:

- A chaotic attractor is a complex phase space surface to which the trajectory is asymptotic in time and on which it wanders chaotically^[13].
- An attractor that shows extreme sensitivity to initial conditions^[14].

Chaotic attractors needn't have an integer dimension like objects which classical geometry would deal with, they can have non-integer or fractal dimensions. In this paper the fractal dimension of a strange attractor is found using the correlation dimension formula (see section 3.6).

A method of quantifying chaotic behaviour is finding the Lyapunov exponent of the system, which is the rate of separation of two neighboring trajectories over time. For a periodic (non-chaotic) attractor the exponent will typically be a non-positive integer, therefore there is another method of checking if a system is chaotic. The rate of divergence of these neighboring trajectories can vary to different initial conditions so there can be a wide range of exponents. It is standard to take the largest of these values, the Maximal Lyapunov exponent because it determines the predictability of the system.

The Lyapunov exponent can also be used to estimate the fractal dimension of the system under analysis. Using the exponent values found the Kaplan-Yorke dimension can be obtained. This dimension is essentially the upper bound for the information dimension.

As mentioned previously, fractals have dimensions which are non-integer, it can often be difficult to analytically obtain the exact dimension however there are multiple mathematical approximations. These result in an array of different dimensions that it's possible to obtain, a list of the more common ones in no particular order is:

- Similarity dimension
- Capacity dimension
- Hausdorff dimension
- Information dimension
- Correlation dimension

The last in this relatively long list is the one of interest in this paper, both because it is well known and because it requires a more reasonable amount of computation to obtain. Although different, each of the dimensions listed have a relationship for example the correlation dimension forms a lower bound for the value of the information dimension. Therefore any result we find for the correlation dimension will be less than or equal to the information dimension of the attractor.

3.3. 5 Non-periodic and periodic behaviour

Taking the logistic map as an example the periodic behaviour observable in dynamic systems can be sampled. A period two sequence will eventually, after transients, yield a series of repeating A,B,A,B,A,B... coordinates, similarly a period four would be A,B,C,D,A,B... etc.

The transient oscillations take the system from the initial conditions to the post transient state^[15]. The oscillating orbits will be attracted to a set of points called the attractor. The data will approach the attractor and as the number of iterations goes to infinity converge on it. Transients should never be recorded as it will be unique to each set of initial conditions and is meaningless. To ensure a chaotic attractor is truly this and not just a set of transient data the number of iterations ignored as transient should be doubled and the attractor obtained should be identical for each set of iterations to infinity. This is also true for periodic attractors, however periodic data is clear to identify immediately and so comparison is unnecessary.

If the system settles down to a periodic orbit of an attractor then it is said to be a periodic attractor, however if no pattern of data emerges the system is behaving chaotically and is said to be a chaotic or strange attractor (when $\lambda = 3.8$ the logistic map has a strange attractor).

It was noted that for some parameter values in dynamic non-linear systems seemingly aperiodic or nonperiodic trajectories can sometimes simply be of very high periodicity, perhaps of a few hundred or thousand iterations^[16] this was mostly overlooked in this paper as the regions with such a high period would be very close to truly chaotic regions. However to ensure that for the attractor which was used to find the correlation dimension the data was plotted using a Fast Fourier Transform (see section 5.5) to examine the chaotic nature fully.

As with the logistic map, even in aperiodic (chaotic) regions a system can be seen to act as periodic orbit when the initial conditions are exactly right to start on an unstable fixed point in the chaotic region. It can be very difficult to predict these values necessary to get this unstable fixed point as even a slight difference will cause the trajectory to quickly iterate away from the unstable fixed point.

It is also possible to force a chaotic region into periodic behaviour, if the initial values are close to an unstable fixed point the system will iterate away from it, however then the system can be 'pushed' back towards the unstable fixed point before the next iteration. Thus iterations can be forced into a periodic behaviour which would naturally be chaotic.

There are also windows inside the chaos, as can be seen in Figure 7 on the following page, which are regions where the parameter values will yield periodic behaviour beyond where the system had initially bifurcated to chaos. These regions of periodicity within an overall chaotic region are called windows. These windows are usually for brief values of the control parameters before bifurcating back to chaos.

3.3. 6 Bifurcation

Still using the logistic map as an example, because it is a simple example, varying λ shows the various periodic orbits possible, if the stable fixed points are plotted on a graph of λ Vs x_{fixed} (Figure 7) a diagram of period doubling bifurcation becomes apparent (where the x_{fixed} coordinates are the x_n values for the fixed points).

When a system shifts from one period to another in this diagram it is said to have undergone a period doubling bifurcation, the period on this diagram splits from period one to period two, two to four, four to eight and so on to period infinity at which point it is chaotic. The length of λ between each of these periods gets less and less as the periodicity gets higher. This period changing all the way to chaos is termed the period doubling route to chaos.

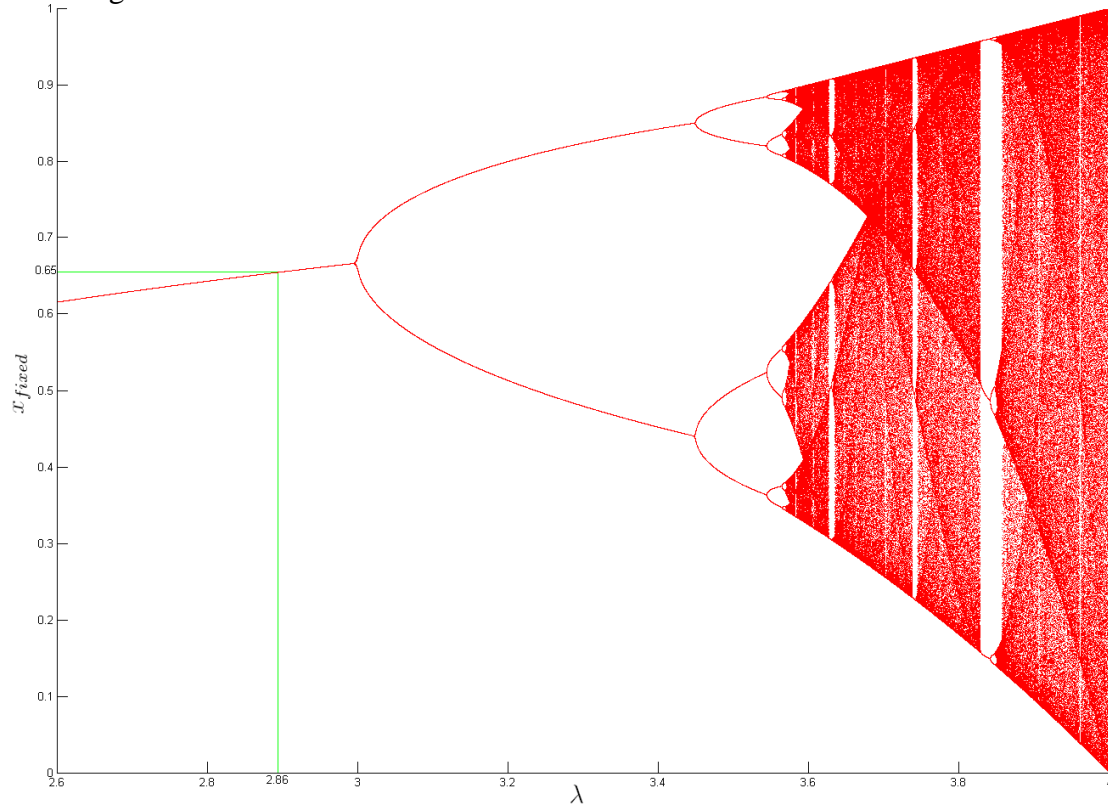


(Figure 7 – Bifurcation diagram for the logistic map generated using Matlab)

The fixed points on the logistic map clearly vary greatly for different values of λ , take an initial value of $x_n = 0.65$ for $\lambda = 2.857142859$, iterating this will return $x_{n+1} = 0.65$ this is because 0.65 is a fixed point for this value of λ . It should be noted that at any fixed point, stable or unstable, if the initial state is exactly the same as the state of the fixed point iterations will always return the same value.

On the diagram the regions where the line splits in two, the bifurcation regions, begin at $\lambda = 3$. When the line splits the previous fixed point becomes unstable (Figure 8) and two new stable fixed points replace the old one. Now, if one of the two fixed points is taken and iterated the result will be the other of the pair of stable fixed points and vice versa. Then when these two lines bifurcate the system has four stable fixed points and to get the starting fixed point four iterations would be necessary.

There are not only periods that are integer powers of two, periodic attractors exist for all odd integers too. In the diagram (Figure 7) windows of periodicity are apparent, in the biggest window there is a region of period three apparent at a λ value of around 3.85. This period three will itself undergo period doubling to chaos, in fact, if we observe a period three oscillations in any system that system is expected to have chaotic regions. It is interesting to note that the bifurcation diagram is an example of a fractal, if you magnify a section of it the self similarity of it is apparent.

The lengths of λ before each period doubling bifurcation gets shorter the higher the period, this observation lead Mitchell Feigenbaum to examine the ratio of these lengths. This will be explained in greater detail in another section (see section 3.5).

When a fixed point bifurcates into two new fixed points the old fixed point becomes an unstable (Figure 8) fixed point which will repel nearby solutions which will be attracted by the local fixed points.

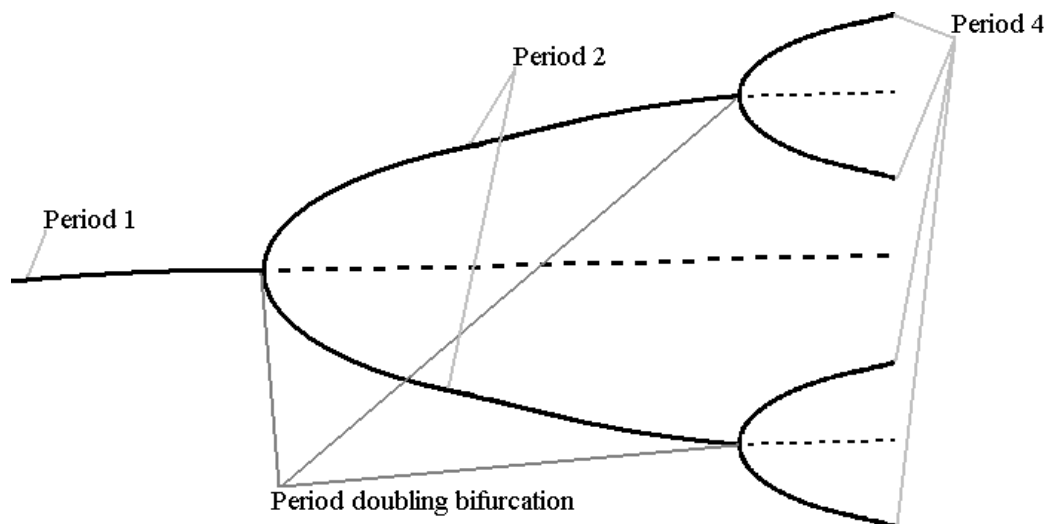


(Figure 8 – Period doubling bifurcations)

As mentioned before even though the unstable fixed points (dotted lines in Figure 8) do not attract x_n values if the initial values are exactly the same as the unstable fixed point then the iterations will remain the same as it. However, if even the slightest change occurs in the values so that they are not exactly equal, then the x_n value will quickly iterate away from it and be attracted to the new fixed points. This behaviour defines unstable fixed points, even the slightest disturbance and the fixed point will be caused to become unstable.

Bifurcations are present in the Rikitake model for various parameter values as will be seen later, very high periods were investigated and the period doubling route to chaos was examined.

3.4 Lorenz Attractor

The Lorenz Attractor is a 3 dimensional structure derived from truncated Rayleigh-Benard equations of convection rolls arising in the fluid dynamics of the atmosphere^[17]. The air is heated by the ground, from its absorption of sunlight, and losses heat into space in the upper atmosphere. Similar to the Rikitake model there are observable regions of periodicity for certain parameter values and regions of chaos for others. The Lorenz equations are also quite similar to those of the Rikitake model:

$$\begin{aligned}\dot{x} &= \sigma(y - x) \\ \dot{y} &= x(\rho - z) - y \\ \dot{z} &= xy - \beta z\end{aligned}\tag{1.6}$$

The overall result is a convective motion, where x represents the convective motion and y and z are the horizontal and vertical thermal variations respectively. The parameters, σ , ρ and β are proportional to the Prandtl number, the Rayleigh number and the size of the system that is being approximated^[18] respectively.

The most important difference between these equations (1.6) and the Rikitake model equations (1.4), is the constant present in the third Rikitake equation^[19]. The reason for examining the Lorenz Attractor is that it is one of the most well documented strange attractors, which make it ideal for cross checking the theoretical accuracy against results of this papers approximated values. For this reason a data set for a specifically well documented Lorenz attractor was found, which was then used to find the correlation dimension of this attractor.

The parameter values for the specific strange attractor used were $\sigma = 10$, $\beta = 8/3$ and $\rho = 28$ ^[20] which was expected to be similar to Figure 9 below.

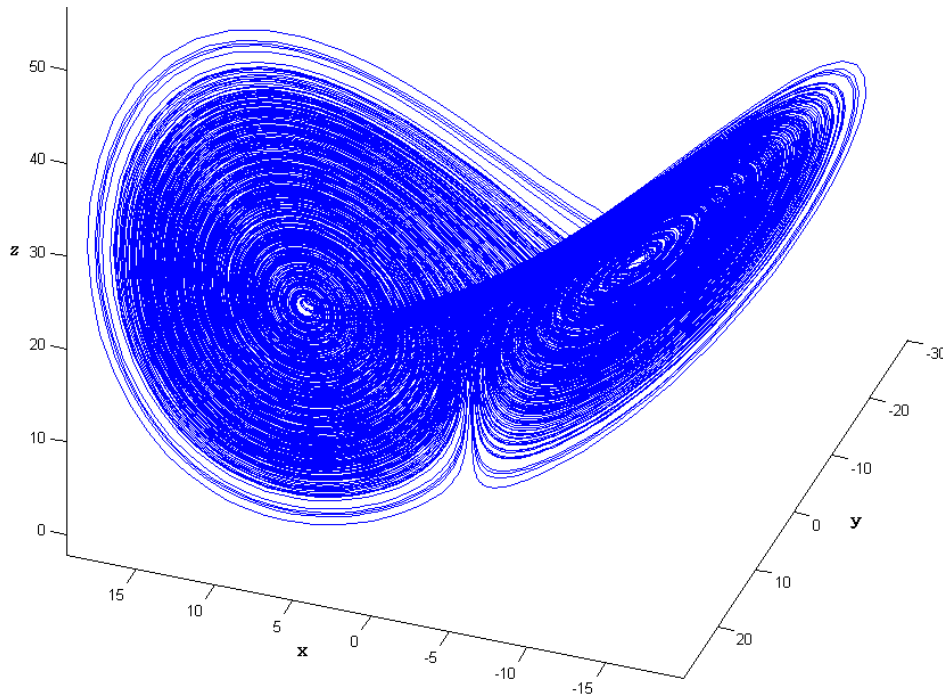


(Figure 9 – Lorenz Attractor 3D plot from MatLab)

Examining a 3-dimensional plot can be difficult, and counting the period even more so. For ease of analysis the return maps were usually plotted in two dimensions and on a large scale, typically multiplying each factor by up to 1000, as in Figure 10 below. Although it is not practical to attempt to count the period of this attractor, as these images are very small, the original size of these images was in the region of 1 square metre which allowed for an in depth view of the structure of the attractor.

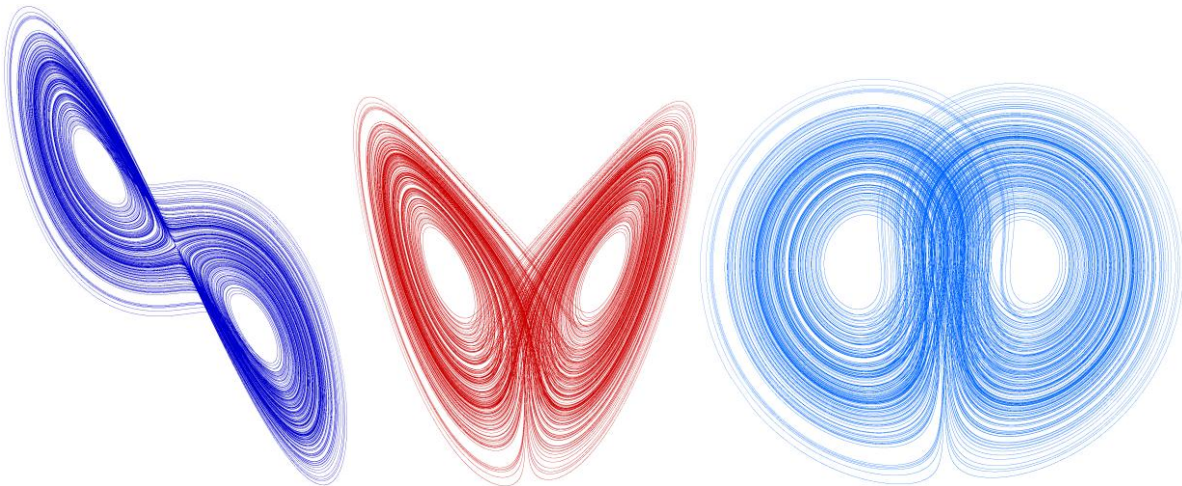


(Figure 10 – High resolution 1-dimension images of the Lorenz Attractor, in the xy, xz and yz planes)

The Lorenz system has a complicated attractor, as seen, with trajectories spiraling around, and oscillating between, two loops^[21], the equations are interesting almost exclusively in the area of chaos analysis and building an understanding of bifurcations and chaotic behaviours which are observed in more and more systems today. Their role in modeling convection has diminished, it being widely accepted that they are only suitable for modeling this at relatively uninteresting parameter values^[22].

It is interesting to note that the system makes many circuits around one of the sides, or lobes, then switches to the other. What's more the number of circuits it makes before changing lobe is dependant on its distance from the centre of that lobe^[23]. Also the amount it exceeds some critical distance of switching determines the point at which it enters the other lobe and the number of circuits it will make before switching back.

Like all dynamic systems, the parameters of the Lorenz equations have certain values which are deemed realistic. It is usual to take the parameters σ and β to be 10 and $8/3$ respectively and to let ρ vary. For values of $\rho < 1$ a stable fixed point of zero is observed, above 1 the system is attracted by two fixed points. These fixed points remain stable for a large range of ρ although at $\rho = 24.74$ they become unstable and the attractor becomes strange^[24]. It should be noted however that for $\rho > 25$ the system is not continuously chaotic, like all chaotic systems there are windows of periodicity throughout the chaotic regions^[25].

3.5 Feigenbaum Constant

As seen from the examples using the logistic map, a dynamical system can bifurcate or period double, eventually doubling to chaos. In 1997 Feigenbaum noted that the pattern of doubling is universal across many systems^[26]. What's more, he mathematically showed that there is a ratio between each region of period doubling which is constant for a very large number of system maps, this ratio is now called the Feigenbaum constant (δ), such that:

$$\delta \equiv \lim_{n \rightarrow \infty} \frac{\mu_{n+1} - \mu_n}{\mu_{n+2} - \mu_{n+1}}$$

$$\delta = 4.6692\dots$$

Where μ_n is normally not the parameter value, μ , which has been discussed previously in terms of the Rikitake model, in this case it is the parameter value location of a bifurcation. So using the logistic map as an example the value for μ_n would be some value of λ at which a bifurcation occurs. The value taken depends on the value of n which is the period of the system at that bifurcation, for example the equation would be the parameter values for period 4 minus period 2, over period 8 minus period 4.

The Feigenbaum constant holds true for all bifurcating systems and can be used to predict the locations of chaotic periods before they ever occur. By using this, knowing the positions of the bifurcation to period 2 and to period 4, the positions of period 8, 16, 32, etc. can be predicted for many systems, including the Rikitake dynamos.

By reexamining the bifurcation diagram (Figure 11) there is a clear scale relationship between period doubling bifurcations, as stated before, the bifurcation diagram is a fractal which means it is self similar through scale. The Feigenbaum constant allows us to use this self similarity to predict regions of periodicity of interest.

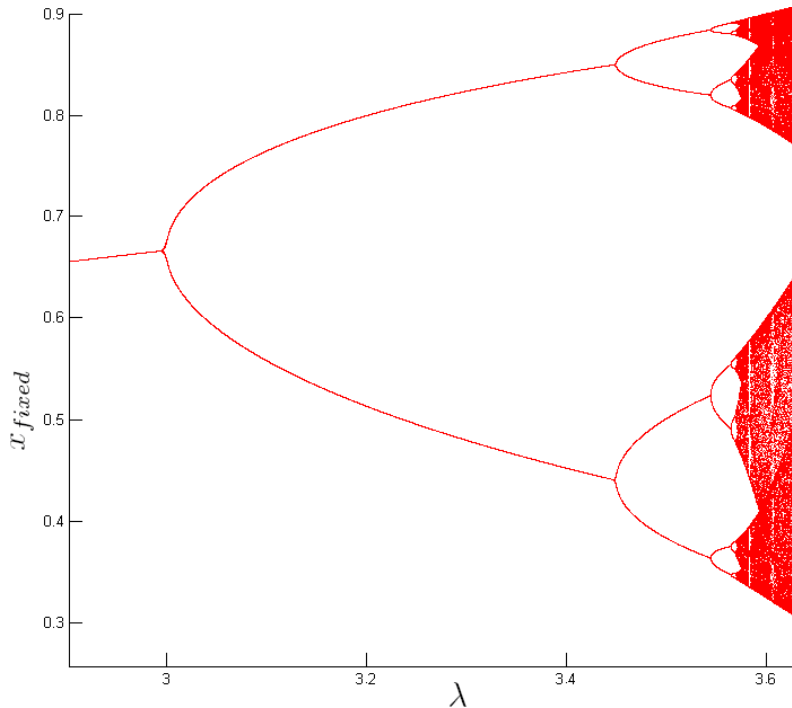


(Figure 11 – Section of bifurcation diagram for the logistic map)

3.6 Correlation Dimension

The correlation dimension is one of many fractal dimensions which can be measured for a given dynamic system. It is presently the most popular measure of dimension^[27]. This is because it is relatively efficient on the amount computation of while probing the attractor to a much finer scale than other measures.

The correlation dimension examines the spatial correlation of points, if two points on the attractor are very close together they are said to be a good approximation of each other and are highly correlated, this dimension ignores time.

The dimension is found by adding the total number of pairs, $n(r)$, of points which are within a certain radius, r , of one another. This is divided by the total number of possible pairs for a data set of size N such that:

$$C_r = \frac{n(r)}{N(N-1)}$$

And $C_r \propto r^{dr}$, where dr is the correlation dimension.

Therefore by taking the log of C_r and r^{dr} and graphing the result the slope of the flat portion of the graph is the correlation dimension as shown below.

$$y = m x + c$$

$$\ln(C_r) = dr \ln(r) + c$$

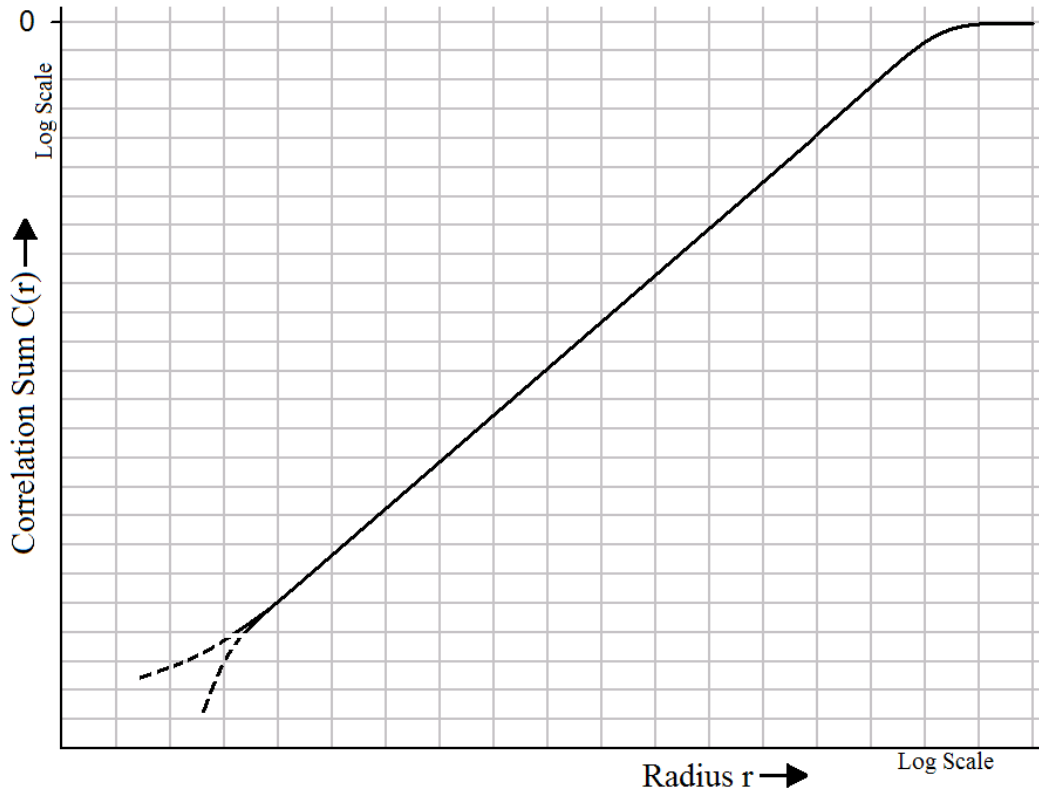


(Figure 12 – Section of bifurcation diagram for the logistic map)

Figure 12 on the previous page shows the type of graph expected from the correlation dimension data obtained. There will be a linear region through the log scale which will yield the slope desired, at either end of this the data will tail off. The reason for this is the size of the radius used.

When r is too large all the pairs begin to be counted, and so when r gets larger again there aren't many more pairs to count such that the growth in number of pairs tails off to 0 as seen in the graph. When r is too small the pair counting is effected in a similar way, the number of pairs counted begins to reach a minimum before finally reaching no pairs counted at all. As the log of zero cannot be taken this point isn't on the graph however the data will tail off towards it.

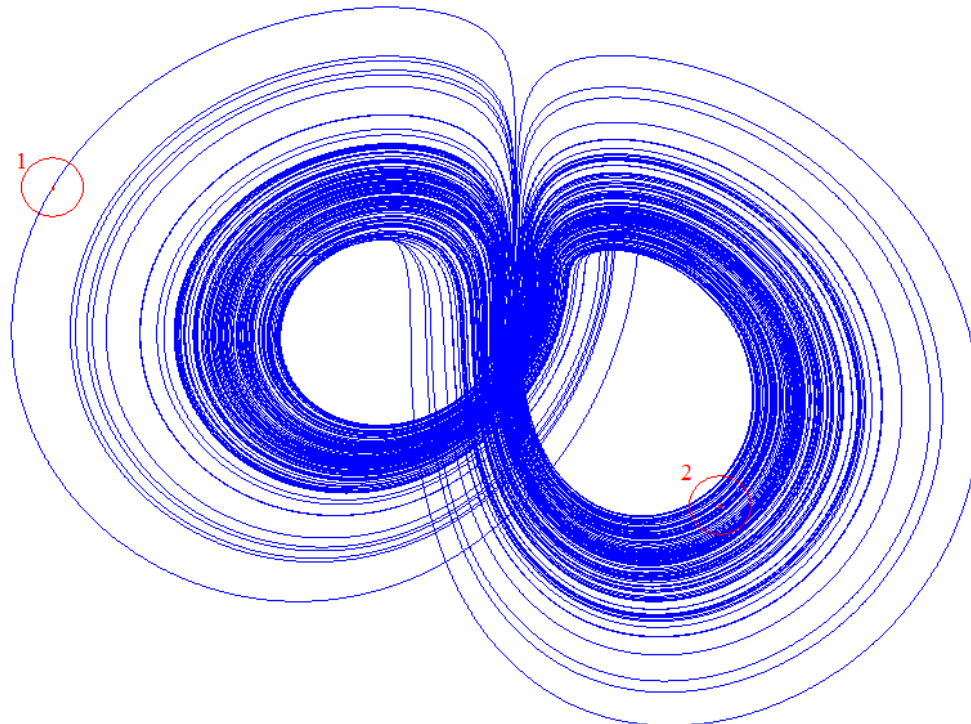


(Figure 13 – 3-dimension plot of a chaotic Rikitake attractor)

In Figure 13 above there are two points drawn which have a radius (r) drawn around them, beginning with point 1 count all of the points inside the radius. There will be a certain number, $n(r)$, of points. Obviously if this is repeated at point 2 the points inside the radius $n(r)$ will be larger and for some point in the centre it could be larger again. Also if r is made large enough every point on the map will be a pair with every other point, and if r is too small no pairs will be counted.

This illustrates the above point which explained the tail regions on the graph, there will be a radius reached at which the entire attractor will be counted and the radii leading to this point will count nearly all of the pairs already which will give very few new pairs to count.

4 Methods:

To fully model the Rikitake dynamos, without computer aid, the time needed would be too large. Although it is possible to directly design circuits to model the system, for this paper the model equations (which were derived and discussed above) were used in a series of C programs. The data from these programs was plotted and examined as a model of the Earth's magnetic field.

In order to fully examine the attractors and time series of the system, for various values of μ and k , multiple C libraries and approaches were used. As this is not the area of interest of this paper not much will be said on it, just to mention that both SDL (Simple DirectMedia Layer) and LibPNG (official C PNG reference library) were utilised to great effect and are recommended for any further study into chaotic attractors using C or C++. Below are two images obtained from SDL (Figure 14) which have been edited together to show the number of period in this plane of the attractor.

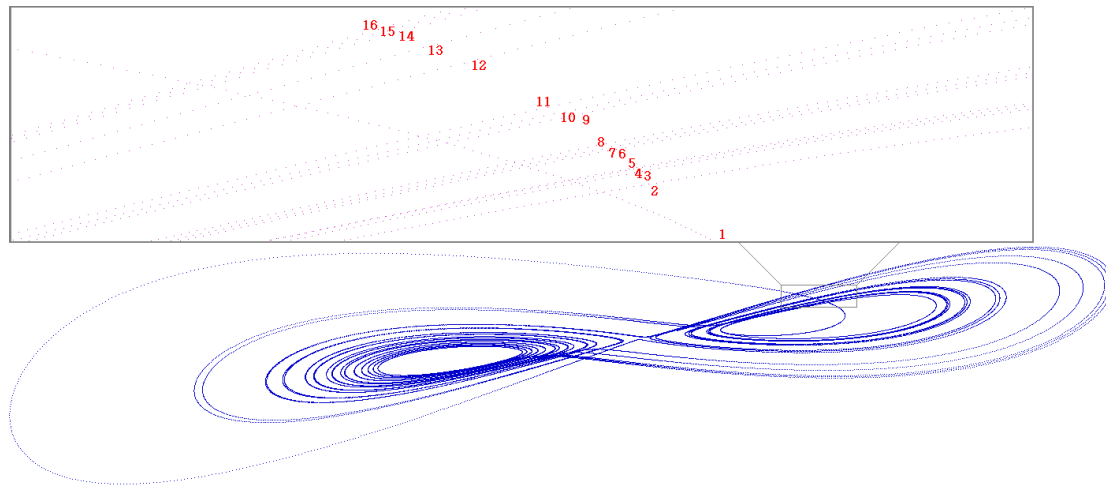


(Figure 14 – Plot of xy plane obtained from C program with SDL library)

A fourth order Runge-Kutta was used to estimate each of the three equations (1.4), this method was used for its high accuracy and relatively low computation time to allow for large data sets to be generated quickly.

Pseudo code:

```
Set initial conditions for  $\mu$ ,  $k$ ,  $X_1$ ,  $X_2$ , and  $Y$ .  
Decide a time step suitable ( $dt \approx 0.0005$ ), and final time ( $t \approx 30000$ ).  
  
For the region of time, in steps of  $dt$ ,  
do a 4th order Runge-Kutta approximation on each equation  
Set the values of  $X_1$ ,  $X_2$  and  $Y$  to the new values.  
  
Outside the transients (to ensure this,  $t_{\text{trans}} \approx 0-29000$ ),  
record the values of  $t$ ,  $X_1$ ,  $X_2$  and  $Y$  to a data file for plotting.
```

Here the data is gathered into a file for plotting or use in another program, a very long transient time was taken to ensure any bounding to the attractor could be examined and avoid gathering the transient data, which would skew results.

5 Results:

5.1 Logistic maps:

From the graphs attached previously (Figures 3 and 4), it was seen that for different λ values even in this simple case that both periodic and chaotic behaviour will emerge in dynamical systems and change depending on the control parameters of the system.

Logistic maps were used in this paper initially to become accustomed to the idea of periodicity, period doubling bifurcations and chaotic behaviours that would be observed in the more complex Rikitake and Lorenz models. It is a very simple method of showing chaotic behaviour as the formula is a simple 1 variable iterative equation.

$$x_{n+1} = \lambda x_n(1 - x_n)$$

There are several features shown in this model which can be hard to demonstrate in other systems, as will be seen in the Rikitake model there are regions of chaos which also have windows of periodicity in them (windows are discussed in section 3.3.6). However these regions in the Rikitake model are hard to analyse as the parameter values they span are very narrow and are in large regions of chaos and so are easy to miss while recording data.

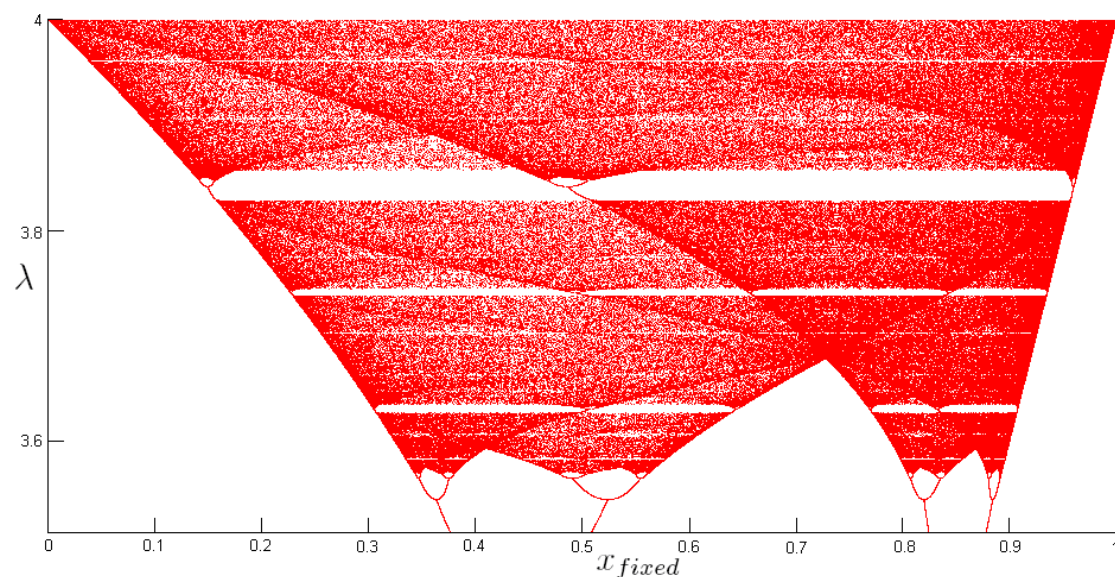


(Figure 15 – Bifurcation diagram for logistic map showing the regions or windows of periodicity within the predominantly chaotic region.)

In the logistic map the windows are relatively easy to find because there is only one control parameter (λ) to vary. These windows demonstrate the behaviour of other systems showing the period doubling bifurcations present even inside the overall chaotic region.

5.2 Lorenz Attractor

Using MatLab a 3-dimensional graph was obtained (Figure 15) for the Lorenz Attractor data collected from the forth order Runge-Kutta approximation. Comparing this to other sources it is clear the data set was correct within reasonable expectations.

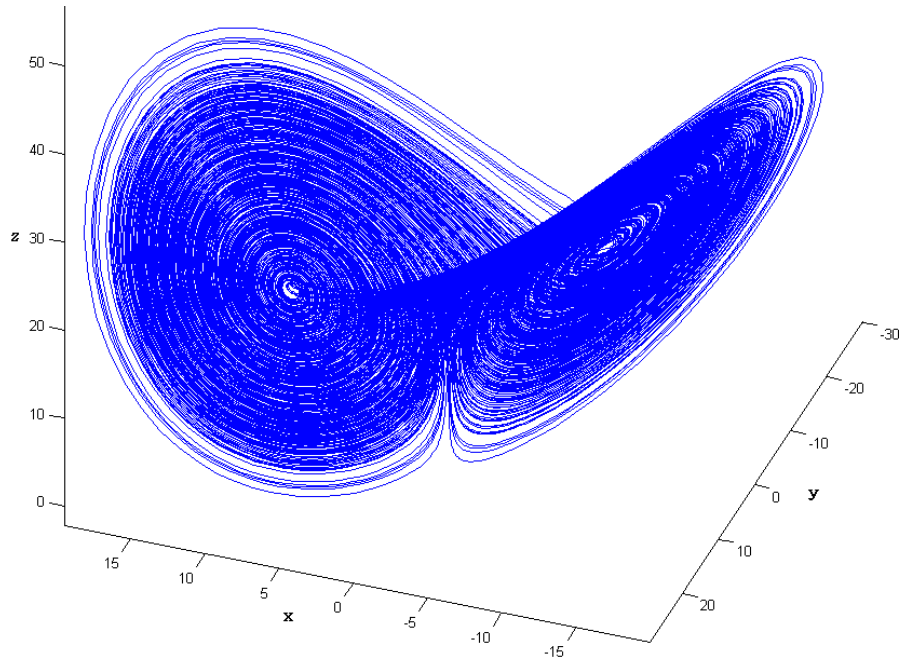


(Figure 15 – Lorenz Attractor from forth order Runge-Kutta approximation data)

Therefore the Lorenz Attractor data gathered is qualitatively similar to that of other sources

Next the data set for this strange attractor was applied to the correlation dimension program, a value had been obtained from a reliable source^[28] for comparison with the model result.

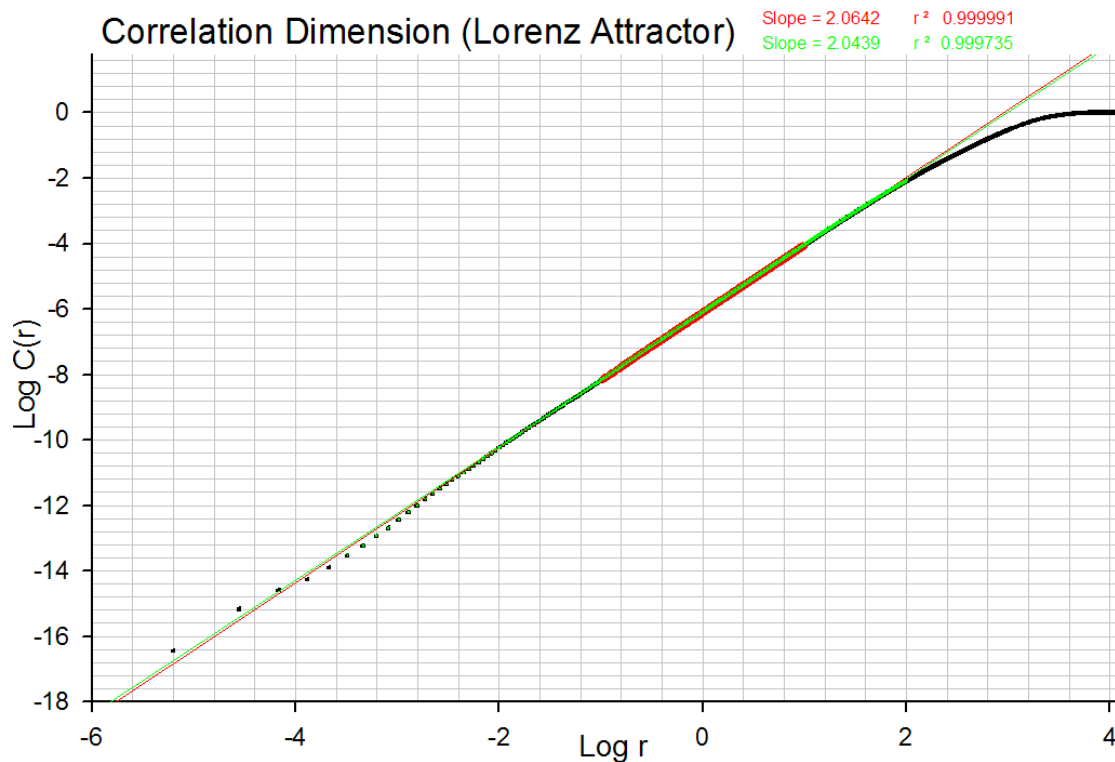


(Figure 16 – Correlation dimension graph for the Lorenz Attractor from forth order Runge-Kutta approximation data)

The two regions in the graph (Figure 16) where the data stops being linear on the log scale are clear on this graph and were ignored in taking the slope. However picking the linear or flat region is difficult to decide accurately, to ensure accuracy a range was taken across the linear region, for two different lengths of the line.

The results of these slopes were $2.0642 \pm 1.9 \times 10^{-5}$ and $2.0439 \pm 5.4 \times 10^{-4}$
Therefore the average of these values with the combined error is $2.05405 \pm 5.59 \times 10^{-4}$

This result is comparable to the expected value for the correlation dimension of the Lorenz Attractor of 2.055 ± 0.004 .

The error stated above for this paper's result is only on accounting for the error in the linear regression and ignores and approximation error.

5.3 Feigenbaum Number

As mentioned previously in section 3.5, the period doubling bifurcations of a system have a pattern, the ratio of one region of a period to the next is a constant named after its discoverer, Feigenbaum. Below is a graph (Figure 17) showing some regions of periodicity and period doubling in the Rikitake dynamo model.

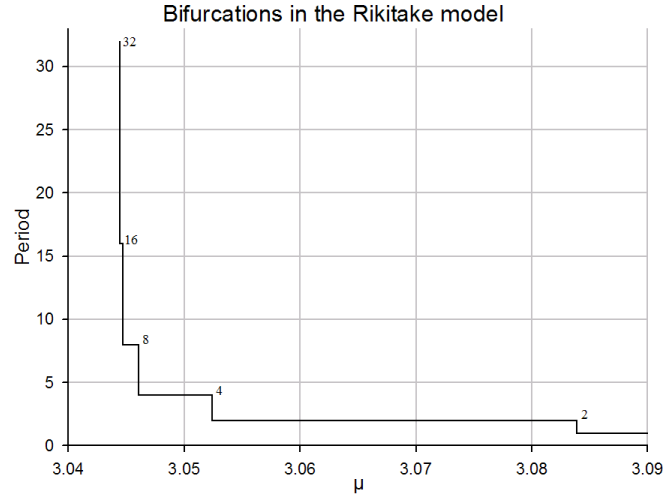


(Figure 17 – Graph illustrating the bifurcations in the Rikitake dynamo over a small region of μ)

The data from this graph is tabulated below (Table 1), between each bifurcation the system remains stable in that period. Due to time limitations the highest period examined was period 32 and only to 4 decimal places, further examination would no doubt reveal further bifurcations eventually leading to chaos.

μ	k	behaviour
3.0444	2.0	Period 32
3.0445	2.0	Period 16
3.0446	2.0	Period 16
3.0447	2.0	Period 8
3.04604	2.0	Period 8
3.04603	2.0	Period 4
3.05239	2.0	Period 4
3.05240	2.0	Period 2
3.08391	2.0	Period 2
3.08392	2.0	Period 1

(Table 1 – Bifurcation locations in μ and k)

$$\delta_{\text{result}} = \frac{\mu_{n+1} - \mu_n}{\mu_{n+2} - \mu_{n+1}}$$

$$\Rightarrow \delta_{\text{result}} = \frac{3.05239 - 3.08391}{3.04604 - 3.05239}$$

$$\Rightarrow \delta_{\text{result}} = 4.96378 \pm 3 \times 10^{-5}$$

$$\delta_{\text{Feigenbaum}} = 4.6692...$$

Although close, this result is well outside the expected error, by finding the location of the bifurcation down to 5 decimal places the error should be almost negligible. However, this does show that the Rikitake model bifurcations obey the ratio Feigenbaum discovered.

5.4 Rikitake Attractors

It should be noted that in the time series graphs and return maps the coordinates were multiplied by some large number before plotting, to magnify the image. In the time series graphs the X1, X2 and Y coordinates were multiplied by 40 and the time scale was multiplied by 5, this meant more of the time series could be viewed while still giving an accurate image however this results in a dissimilarity with any repeated data unless it follows the same multiplication ratio.

In the return maps the coordinates were multiplied by 60, 80 or 100 depending on the size of the map before multiplication, provided each variable has the same multiple this will not effect the overall look of the maps.

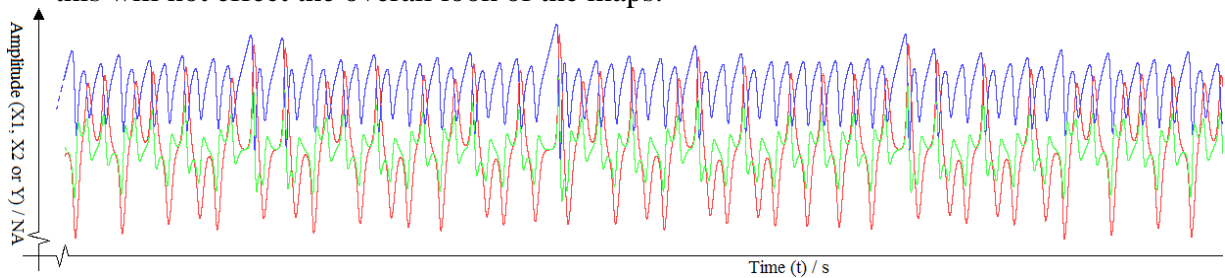


(Figure 18 – Example time series graph for parameter values $\mu = 0.7$ and $k = 2.0$)

Figure 18 shows an example of how the time series graphs were unedited, to get a clearer picture each of the three variables, X1 being red, X2 being green and Y being blue, were plotted separately. The example above is from a chaotic region.

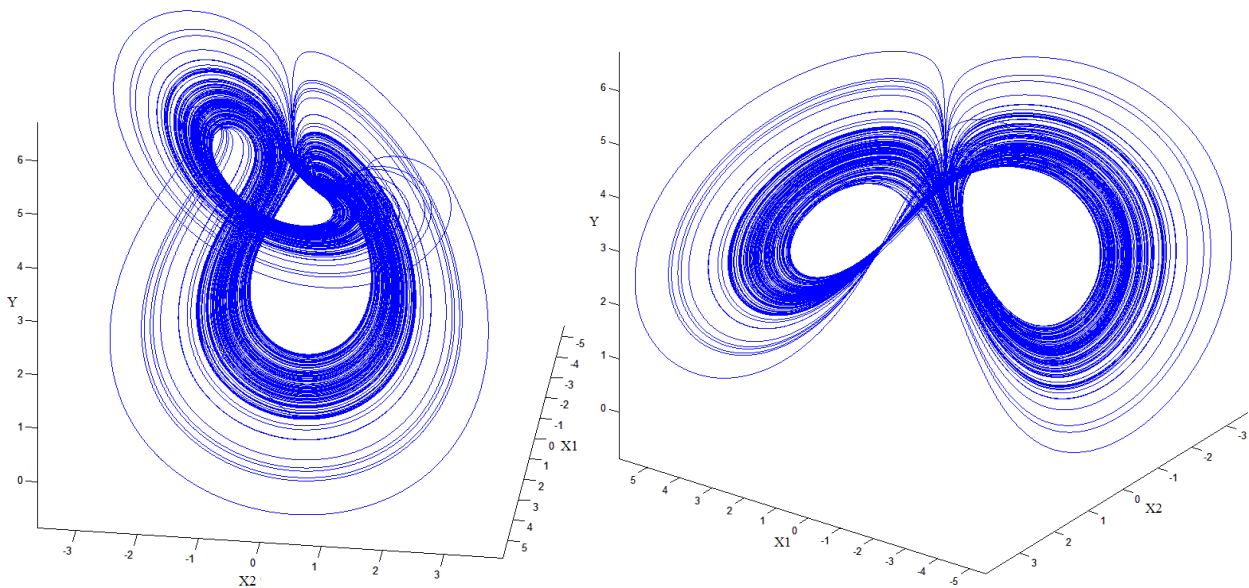


(Figure 19 – 3-dimensional graphs of a strange attractor from the Rikitake model, $\mu = 0.7$ and $k = 2.0$)

As with the Lorenz Attractor Matlab was utilised to generate 3-d graphs of a strange attractor from the Rikitake model (Figure 19), it was noted that for varied values of μ and k there were various shapes the attractor could take. They all roughly kept the same twisted loop structure but there were a range of sizes and degrees of twists.

N.B. More 3-d plots, time series graphs and return maps are attached in the appendix for further examination of the Rikitake attractors.

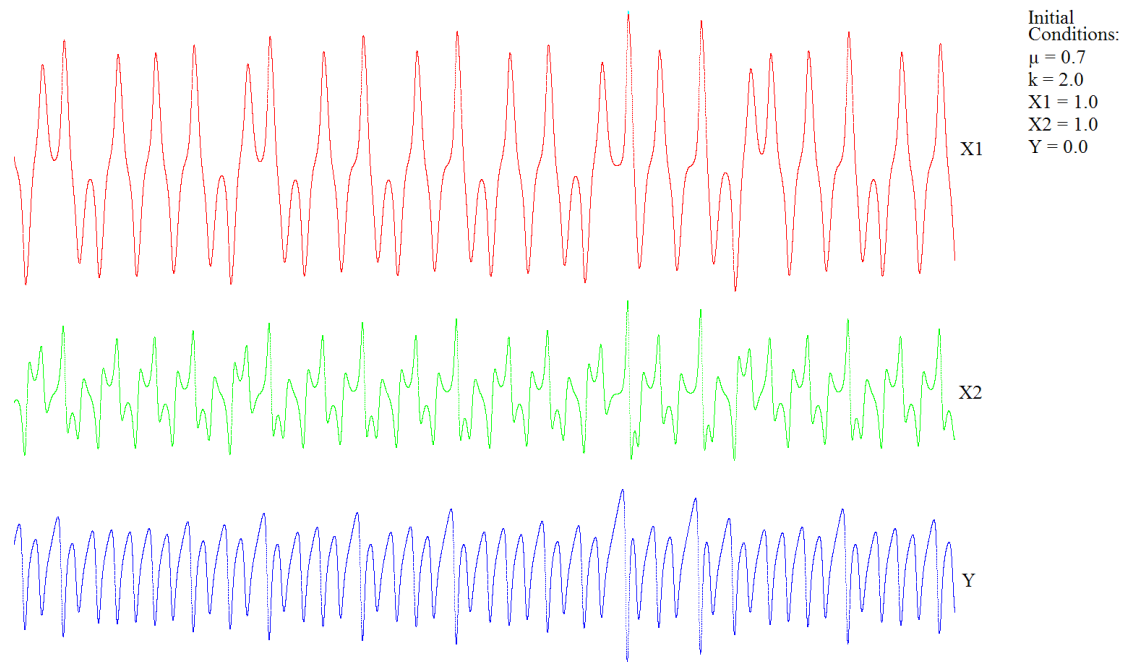


(Figure 20 – Time series graph showing chaotic data)

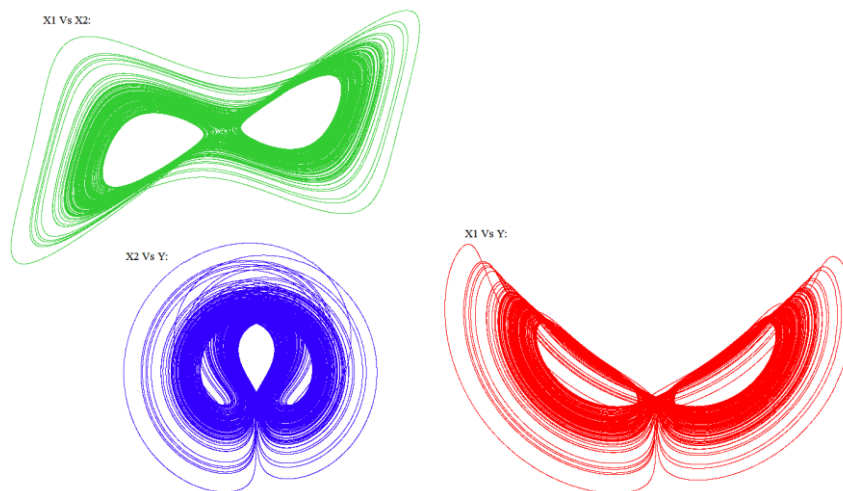


(Figure 21 – Return maps plotted from the above time series showing 1-d views of the attractor)

Figures 20 and 21 above show the time series and return maps plotted for the attractor shown in Figure 19, the return maps clearly show chaotic behaviour, however the time series does have an almost periodic looking structure, therefore it was noted to avoid drawing conclusions based singularly on either of the sources.

It was also noted that there is a clear similarity between the Lorenz Attractor and the observed Rikitake strange attractors, this is not very surprising as it was already mentioned that their equations are quite similar although the observed similarity does give more confidence to results of this model.

To show a clear difference between the chaotic and periodic behaviours of the model a period 1 region was graphed (Figures 22 and 23).

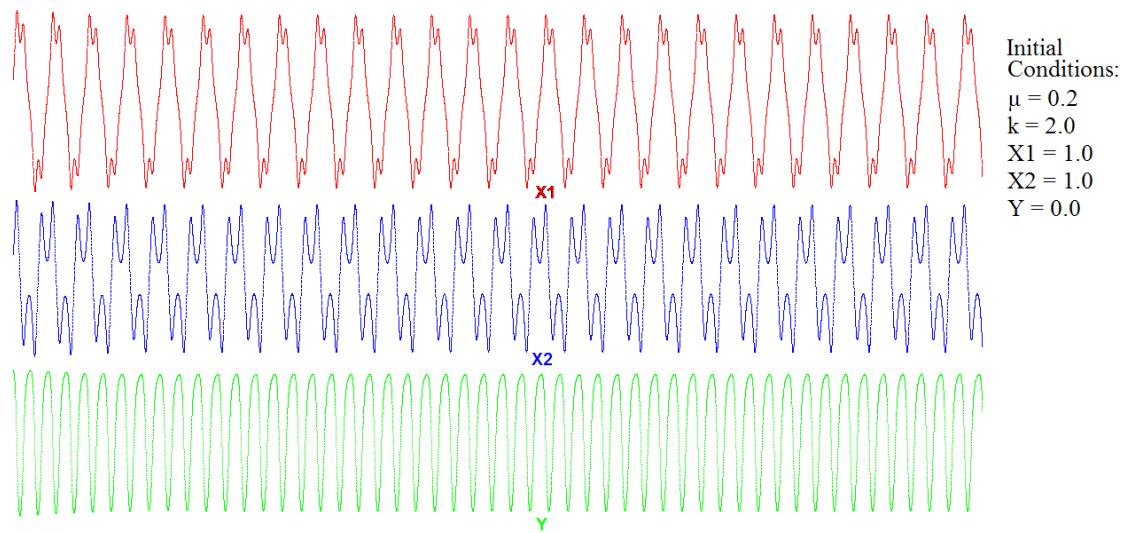


(Figure 22 –)

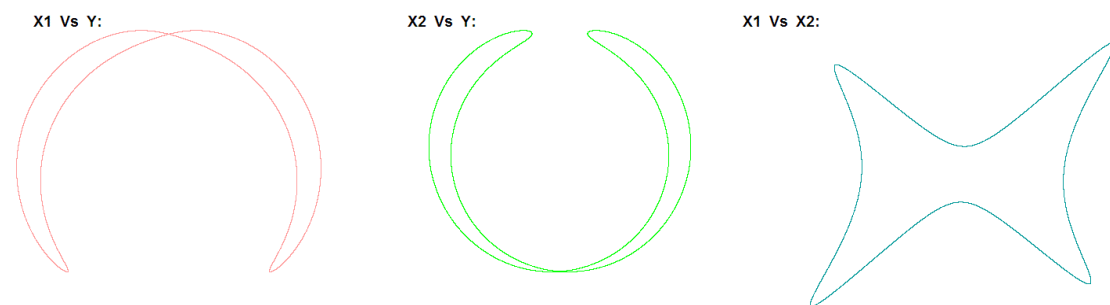


(Figure 23 –)

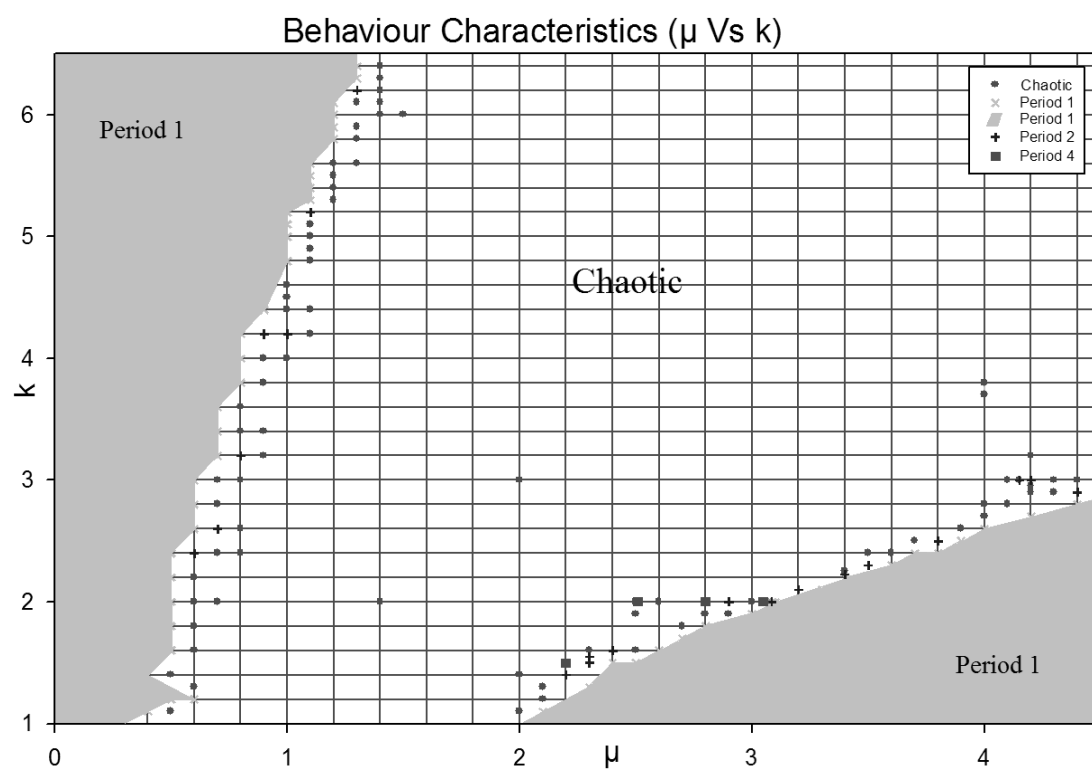


(Figure 24 – Map of the behaviour characteristics of the Rikitake model for various parameter values, similar to the bifurcation diagram)

5.5 Correlation Dimension

As discussed in section 3.6 the areas above and below the flat region (Figure 25), are due to the value of the radius, r , being too small or too large which causes miscounting of pairs, as when r is too small the number of pairs approaches zero as no neighboring points are within the radius and when r is too large the number of pairs approaches the number of total pairs (where the graph reaches $\text{Log } C(r) = 0$). Therefore the data at either end where the curve tails off must be ignored.

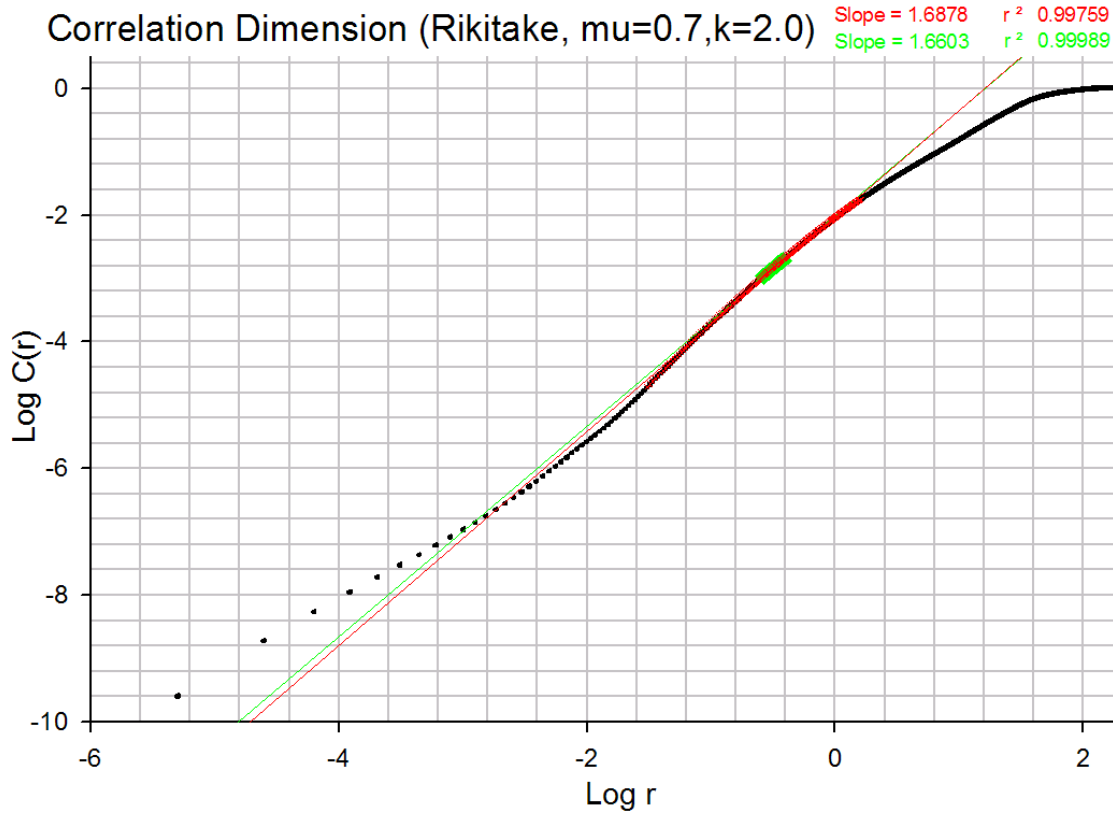


(Figure 25 – Correlation dimension graph for a strange attractor of the Rikitake model)

The results of these slopes were $1.6878 \pm 4.07 \times 10^{-3}$ and $1.6603 \pm 1.83 \times 10^{-4}$
Therefore the average of these values with the combined error is $1.67405 \pm 4.25 \times 10^{-3}$

The error stated above is only on accounting for the error in the linear regression and ignores and approximation error which is very low for a fourth order Runge-Kutta with a small step size.

6 Discussion:

Firstly to discuss one major feature which was noted while gathering data on the Rikitake model was the limits on the values of μ and k . As noted previously they have certain realistic values for the Earth, μ of the order 10^{-3} to 10^1 and $k = 2$. However, while modelling the system for large values of μ and k , the sum of the two greater than roughly 8.0, then the model values would iterate to infinity very quickly yielding no non-transient result data. This finding could not be confirmed by other sources on the model, however the same code yielded the Lorenz Attractor correlation dimension relatively accurately and several programs were written to cross check the data including using second order Runge-Kutta and Euler approximations, all of which returned the same exponential increase in values after very few iterations.

Because of this and other noted points it became necessary to write several programs more than first anticipated; to get an idea of data sets a second order Runge-Kutta (in C) was first used to approximate the results of the equations, for similar reasons the data was found using Euler's method (in C and Python).

A fourth order Runge-Kutta (in C and Python) was used as the main generator of data sets, as its accuracy was desirable, it was used for both Rikitake and Lorenz equations. To plot the data it was necessary to utilise two C libraries, SDL and LibPNG, to deal with the very large data sets generated (roughly 1 million points in 3 dimensions with time), it would have been possible to use several plotting programs although it was found that most of them struggled with such a large quantity of data.

Finally a code to find the correlation dimension was used for several of the data sets gathered from both Lorenz and Rikitake equations. This code was the most time consuming (around 7 hour runtimes depending completely on the data set size) with no noted way to decrease runtime other than use smaller data sets which effects the overall accuracy (by covering only one lobe of the attractor for example).

The reason Python was used to code the programs as well as C was due to a truncation issue which was noticed with C. Most of the data collected was stored in plain text format for various plotting operations and further use in programs, when these files were written by C the numbers would be truncated to 6 decimal places regardless of significant figures, which meant when the values approached zero but where still non-zero the data was reading as zero. In Python however the data would be recorded with an exponential power for very large or very small values.

Excel Spreadsheet was also used to approximate the data, only simple short data sets could be generated for the Rikitake or Lorenz equations, however almost all of the logistic map data was generated using Excel as it is such a simple calculation and the transients typically doesn't last for more than 500 iterations.

The disc dynamo models suggest that the Earth's magnetic field is generated by the flow of electricity in the molten iron outer core of the Earth^[1], other models include various other factors which influence the Earth's magnetic field, however the Rikitake model is both simple and elegant in that it models the chaotic reversals while still being possible to model using a dimensionless 3 equation program. There are simpler models however, but these do not typically display the chaotic reversals observed in this model.

It has been shown that the synchronisation of chaotic systems has many potential applications in laser physics, chemical reactors, secure communication and biomedical systems^[2]. As briefly mentioned before a chaotic system can be forced to have periodic behaviour, this can be important in generating future technologies as processes need to be periodically repeatable for most applications.

Chaos theory is observable all around us in nature, and fractal dimensions can be used to describe a great many natural and man-made

7 Conclusion:

Unfortunately due to time taken up investigating the limits of μ and k , as well as trouble designing a program which minimised computation time while giving an accurate result for the correlation dimension, the Lyapunov exponent of the Rikitake strange attractor was not investigated. It was also planned that the Fast Fourier Transforms of chaotic and periodic data would be included, however it proved difficult to obtain this data despite repeated attempts.

Further time to continue this paper was desired, the behaviour of the model for certain values of μ and k created many more questions and the chaotic behaviour could be analysed further.

Chaotic reversals were observed for certain parameter values of μ and k within the limits deemed realistic for the Earth. This shows that for certain initial states of the Earth's geodynamo and magnetic field the polarity switches would be chaotic about two fixed points.

The results of the test on the model accuracy using the correlation dimension of the Lorenz Attractor show that the model is accurate to a good degree. This adds confidence to the model of the Rikitake two-disc dynamo both for the quantitative and qualitative results.

The model showed chaotic behaviour about two fixed points and the correlation dimension of the strange attractor for a region within the limits, $\mu = 0.7$ and $k = 2.0$, was found to be 1.67405 ± 0.00425 . This dimension is clearly a non-integer, i.e. a fractal, which quantitatively supports that the attractor is chaotic.